

## A phase detection method for visualizing single- and bilayer graphene on a SiC surface

© A.D. Rodionchikova, M.S. Dunaevskiy, E.V. Gushchina, S.Yu. Priobrazhenskii,  
S.P. Lebedev, A.A. Lebedev

Ioffe Institute, St. Petersburg, Russia  
E-mail: a.rodionchikovaa@mail.ru

Received October 2, 2025

Revised November 22, 2025

Accepted November 23, 2025

A phase detection method for visualizing single- and bilayer graphene regions on a SiC surface is proposed. The phase detection method demonstrates a lateral resolution of 5–10 nm, significantly higher than that of the traditional Kelvin probe microscopy method. The single-pass phase detection method significantly accelerates image acquisition and reduces the risk of probe tip degradation.

**Keywords:** scanning probe microscopy, Kelvin probe microscopy, phase detection method, graphene, bilayer graphene, silicon carbide.

DOI: 10.61011/TPL.2026.03.63067.20513

Two-dimensional materials, such as graphene, transition metal dichalcogenides, hexagonal boron nitride, etc., have recently attracted considerable research attention. Graphene, which is one of the most promising materials of this class, holds a special place among them [1]. The capacity to synthesize graphene on large-sized substrates is crucial for production of graphene-based device structures. The most common method is high-temperature annealing of SiC crystals, which results in the formation of both single-layer (1L) and bilayer (2L) graphene regions on the Si face [2]. An important applied problem is the optimization of growth parameters (temperature and annealing duration) with the aim of minimizing the amount of bilayer graphene on the surface. Kelvin probe microscopy (KPM) is traditionally used to visualize the distribution of single-layer and bilayer graphene regions, since their corresponding surface potential values differ by 130 mV [3]. However, this method has a significant drawback: the lateral resolution is insufficient [3], which is attributable to the long-range nature of the electrostatic interaction. This may lead to inaccurate measurement of the number of bilayer graphene regions on the surface. In addition, the two-pass scanning mode makes measurements fairly slow, reducing the efficiency of KPM. In the present study, we propose an alternative approach (phase measurement in the tapping mode) that visualizes monolayer and bilayer graphene regions as well, but does so faster and with a higher lateral resolution. It is also demonstrated that the phase detection method differs from KPM in being less sensitive to the type of probes used.

Silicon carbide (polytypes 4H-SiC and 6H-SiC) samples annealed at characteristic temperatures of 1800 °C [2] were examined. With such annealing, approximately 30% of the Si face is covered with 2L-graphene, and the remaining part of the surface is covered with 1L-graphene. Regions with 1L- and 2L-graphene were chosen on these samples

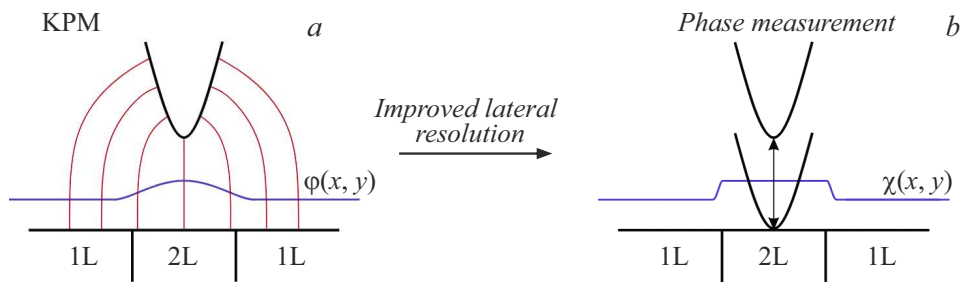
and scanned simultaneously using the KPM method and the phase detection method (PDM) in the tapping mode. The obtained images were analyzed to determine the lateral resolution of KPM and PDM.

KPM (Fig. 1, *a*) is a traditional method for measuring surface potential  $\varphi(x, y)$  [4]. The phase detection method (Fig. 1, *b*), which is implemented in the tapping mode, relies on detection of the phase shift of oscillations of a probe induced by its interaction with the surface. In this mode, the probe undergoes periodic oscillations, touching the sample at the lowest point. At the moment of contact, the probe is affected by short-range forces, which include repulsive and adhesion ones and may induce a phase shift in probe oscillations. This change  $\chi(x, y)$  is recorded in the device memory.

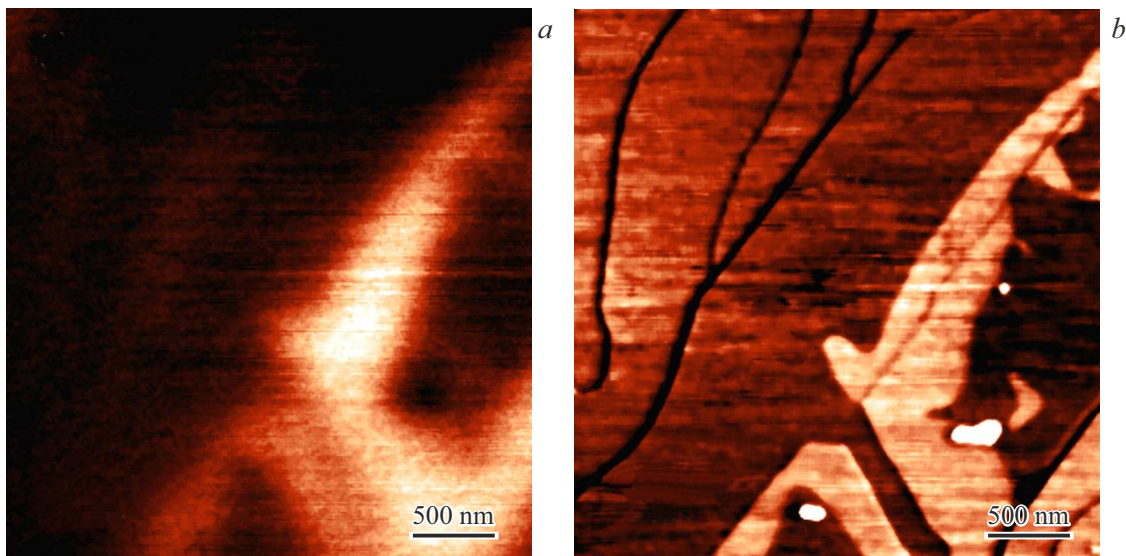
Measurements were performed with an NTegra-Aura (NT-MDT, Russia) scanning probe microscope (SPM). HA-FM probes (TipsNano, Russia) and similar HA-FM/W2C probes with a conductive W<sub>2</sub>C coating (TipsNano, Russia) [5] were used in the study. Measurements were carried out in the two-pass mode: the topography and PDM phase were recorded in the first pass, and the potential was measured by KPM in the second pass. The approximate probe–surface distance in the second pass was 30–40 nm.

Figure 2 shows SPM images of single-layer and bilayer graphene regions on the SiC surface obtained by KPM (*a*) and the phase detection method (*b*). Comparing them, one sees that the KPM method blurs the boundaries of 2L-graphene, while phase detection allows one to visualize the regions clearly.

The blurring of boundaries in KPM is attributable to the fact that oscillations of a probe in the process of scanning are affected not only by the potential of the local region located directly below it, but also by the potential of adjacent regions. The instrument function of KPM



**Figure 1.** Diagram of the experiment. *a* — Potential measurement by KPM; *b* — phase measurement (PDM).



**Figure 2.** SPM images of graphene on a SiC substrate obtained using KPM (*a*) and the phase detection method (*b*). A HA<sub>2</sub>FM probe was used for measurements.

depends on the probe type and the probe–surface distance. According to literature data, its lateral resolution varies widely (from several tens to hundreds of nanometers) [6,7]. In theory, the finest lateral resolution is achieved at minimum probe–surface distances [8]. However, the effective resolution in actual experiments rarely exceeds 50–100 nm (especially when probes with a conductive coating required to detect the KPM signal are used), which is consistent with our experimental data presented in Figs. 2 and 3. Note that two-pass operation at short distances is extremely risky, since the probe may penetrate the surface during the second pass due to imperfect operation of the two-pass mode. In addition, probes with a conductive coating need to be used in KPM to enhance the recorded signal. This coating increases the probe tip radius by 20–30 nm and has a negative effect on lateral resolution.

Unlike KPM, the phase detection method has a narrower instrument function (Fig. 3) that does not depend on the probe type and the distance to the surface. Its lateral resolution is determined by the size of the contact area in the tapping mode and is 3–5 nm [9].

The measured potential and phase profiles are a convolution of measured object  $h(x)$ , which is a sharp step, and instrument function  $A(x)$ :

$$h_{meas}(x) = h(x) * A(x), \quad (1)$$

where the asterisk denotes convolution. It is possible to extract data on the instrument function by differentiating the measured step (KPM or PDM) [10]. Accurate determination of the instrument function and lateral resolution requires fine-step measurements and numerical differentiation of noisy profiles. The signal–noise ratio normally deteriorates after differentiation, necessitating smoothing or Gaussian approximation. In the present study, we used a simpler method for determining the lateral resolution: measurement of the width of a step at 25 and 75% of its full height (see marks on the profiles in Figs. 3, *c* and *d*). This interval corresponds approximately to the width at half maximum of the instrument function, which allows one to estimate the lateral resolution.

It should also be noted that the lateral resolution in KPM depends to a significant extent on the type of probe and its

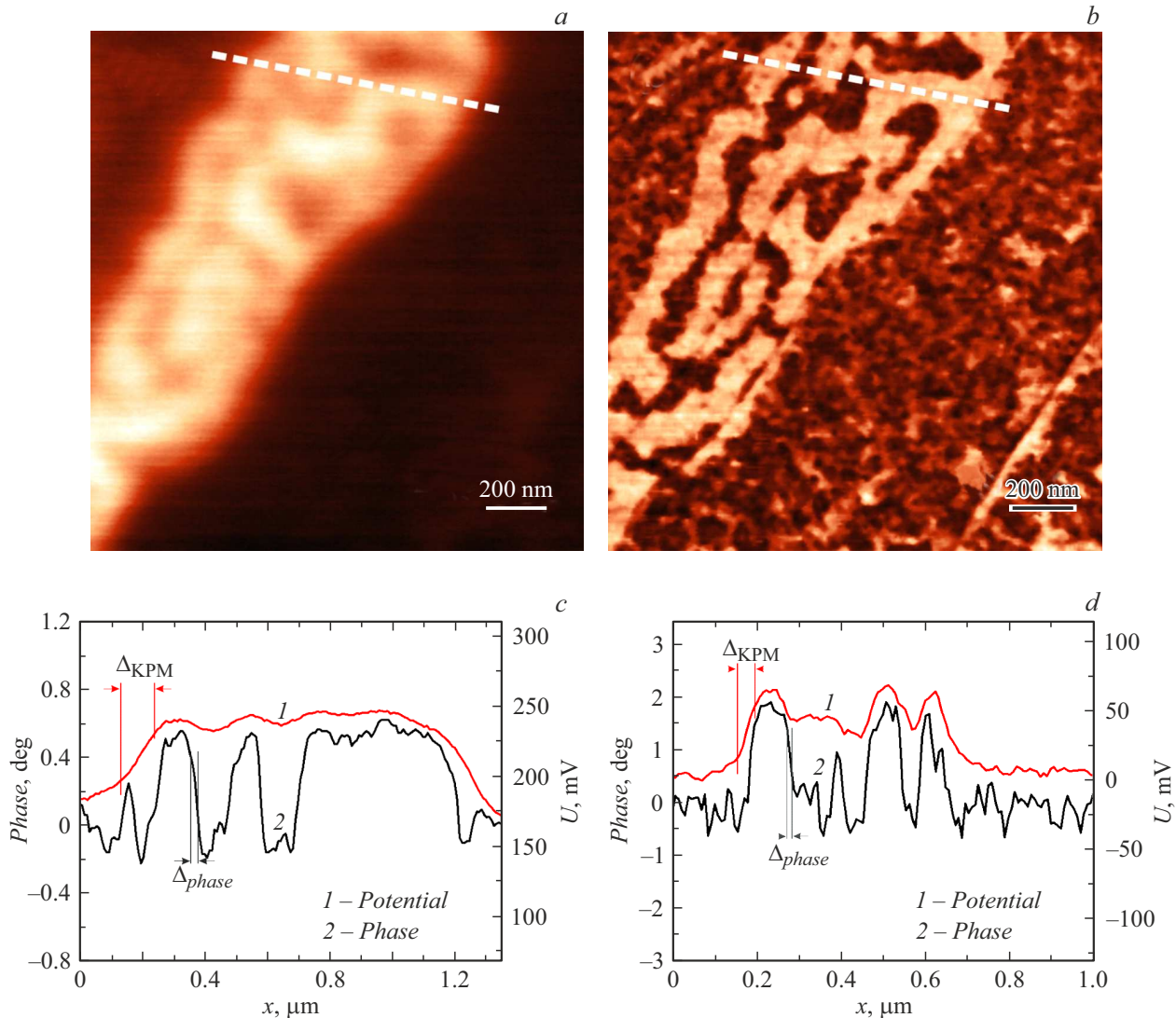


**Figure 3.** *a* — KPM image of the graphene surface; *b* — PDM image of the graphene surface; *c* — graphene surface profiles (marked with dashed lines in panels *a* and *b*) obtained by a probe with an HA\_FM/W2C coating; *d* — graphene surface profiles obtained by a probe without an HA\_FM coating. Step widths corresponding to the lateral resolutions of KPM and PDM are indicated in the profiles shown in panels *c* and *d*).

coating. Probes with conductive coatings (Pt, Au, PtIr, W<sub>2</sub>C, etc.), which allow for amplification of the recorded signal, are often used for KPM measurements. The use of probes with a conductive W<sub>2</sub>C coating (HA\_FM/W2C probes) increases the tip curvature radius from 10 nm (for probes without an HA\_FM coating) to 35 nm, reducing the lateral resolution significantly (down to 50–100 nm). In contrast to KPM, the sensitivity and resolution of the phase detection method are virtually independent of the type of probe and its coating. In support of this thesis, we performed comparative measurements of 1L- and 2L-graphene regions by KPM and PDM using HA\_FM and HA\_FM/W2C probes with the same geometric parameters, the difference being that the latter probe has a W<sub>2</sub>C conductive coating. Figures 3, *a* and *b* present the images obtained by the coated probe. As in Fig. 2, one sees clearly that the

boundaries of bilayer graphene are blurred in the KPM measurement, while PDM ensures their clear identification. Moreover, the phase detection method demonstrates equally high clarity of boundaries in measurements with uncoated (Fig. 2, *b*) and coated (Fig. 3, *b*) probes, confirming that the PDM resolution does not depend on the probe type. Figures 3, *c* and *d* present cross sections of the surface potential and phase profiles obtained using coated and uncoated probes, respectively. All images obtained by the phase detection method have sharp boundaries, while profiles measured by KPM are characterized by a significant broadening of features and loss of detail. When an uncoated (HA\_FM) probe was used in phase detection measurements, the step width was  $\sim 10$  nm; in KPM measurements, this value increased to 50 nm. The KPM resolution deteriorated further following the transition to a

probe with a conductive coating (HA\_FM/W2C): the step width increased to  $\sim 100$  nm. Thus, coupled with various types of probes, PDM provides several times higher lateral resolution than KPM.

The obtained results demonstrates that the phase detection method has significant advantages over Kelvin probe microscopy in characterization of graphene layers on SiC. Being a single-pass technique, PDM provides higher lateral resolution that is independent of the probe type, allowing for rapid and clear visualization of the boundaries between monolayer and bilayer graphene. Precise determination of the shape and size of monolayer and bilayer graphene regions on SiC substrates makes PDM the method of choice for such measurements. It should be noted that the proposed technique is most efficient in the analysis of objects with known morphology, such as the specially prepared samples with 1L- and 2L-graphene regions considered above. If the morphology of examined objects is not known, it becomes significantly harder to interpret the obtained data; however, morphology may serve as a key criterion for their identification: crystalline inclusions normally feature pronounced faceting, while impurity regions are characterized by rounded and blurred boundaries.

### Conflict of interest

The authors declare that they have no conflict of interest.

### References

- [1] A.R. Urade, I. Lahiri, K.S. Suresh, *JOM*, **75** (3), 614 (2023). DOI: 10.1007/s11837-022-05505-8
- [2] A.A. Lebedev, S.Yu. Davydov, I.A. Eliseyev, A.D. Roenkov, O. Avdeev, S.P. Lebedev, Yu. Makarov, M. Puzyk, S. Klotchenko, A.S. Usikov, *Materials*, **14** (3), 590 (2021). DOI: 10.3390/ma14030590
- [3] S.P. Lebedev, I.A. Eliseyev, M.S. Dunaevskiy, E.V. Gushchina, A.A. Lebedev, *C — J. Carbon Res.*, **9** (3), 62 (2023). DOI: 10.3390/c9030062
- [4] A. Zahmatkeshsaredorahi, D.S. Jakob, X. Xu, *J. Phys. Chem. C*, **128** (24), 10289 (2024). DOI: 10.1021/acs.jpcc.4c01461
- [5] TipsNano.ru [Electronic resource]. <https://tipsnano.ru>
- [6] M. Nonnenmacher, M.P. O'Boyle, H.K. Wickramasinghe, *Appl. Phys. Lett.*, **58**, 2921 (1991). DOI: 10.1063/1.105227
- [7] W. Melitz, J. Shen, A.C. Kummel, S. Lee, *Surf. Sci. Rep.*, **66**, 1 (2011). DOI: 10.1016/j.surfrep.2010.10.001
- [8] D. Ziegler, P. Gava, J. Guttinger, F. Molitor, L. Wirtz, M. Lazzeri, A.M. Saitta, A. Stemmer, F. Mauri, C. Stampfer, *Phys. Rev. B*, **83**, 235434 (2011). DOI: 10.1103/PhysRevB.83.235434
- [9] K. Bian, C. Gerber, A.J. Heinrich, D.J. Müller, S. Scheuring, Y. Jiang, *Nat. Rev. Meth. Primers*, **1** (1), 36 (2021). DOI: 10.1038/s43586-021-00033-2
- [10] M.S. Dunaevskiy, E.V. Gushchina, D.A. Malykh, S.P. Lebedev, A.A. Lebedev, *Tech. Phys. Lett.*, **49**, 238 (2023). DOI: 10.1134/S1063785023900133.

*Translated by D.Safin*